Shape of the Retinal Surface in Emmetropia and Myopia

David A. Atchison,[1] *Nicola Pritchard,*[1] *Katrina L. Schmid,*[1] *Dion H. Scott,*[1] *Catherine E. Jones,*[2] *and James M. Pope*[2]

Purpose. To determine and compare the shapes of the retinas of emmetropic and myopic eyes.

Methods. Nonrotationally symmetrical ellipsoids were mathematically fitted to the retinal surfaces of 21 emmetropic and 66 myopic eyes (up to −12 D) of participants aged 18 to 36 years (mean, 25.5) using transverse axial and sagittal images derived from magnetic resonance imaging.

Results. The shapes of the ellipsoids varied considerably between subjects with similar refractive errors. The shapes were oblate (steepening toward the equator) in most of the emmetropic eyes (i.e., the axial dimensions of the ellipsoids were smaller than both the vertical and horizontal dimensions). As myopia increased, all ellipsoid dimensions increased with the axial dimension increasing more than the vertical dimension, which in turn increased more than the horizontal dimension (increases in approximate ratios 3:2:1). The relative difference in the increase of these dimensions meant that as the degree of myopia increased the retinal shape decreased in oblateness. However, few myopic eyes were prolate (flattening toward the equator). Independent of myopia, the ellipsoids were tilted about the vertical axis by 11° ± 13°, and ellipsoid centers were decentered horizontally by 0.5 ± 0.4 mm nasally and 0.2 ± 0.5 mm inferiorly, relative to the fovea.

Conclusions. In general both emmetropic and myopic retinas are oblate in shape, although myopic eyes less so. This finding may be relevant to theories implicating the peripheral retina in the development of myopia. (*Invest Ophthalmol Vis Sci.* 2005; 46:2698–2707) DOI:10.1167/iovs.04-1506

From the late 1940s, ocular size and shape have been described or inferred by a variety of techniques such as entopic phenomena,[1] x-ray tomography,[2] A- and B-scan ultrasound,[3,4] optical coherence reflectometry,[5] and peripheral refraction.[6–8] Magnetic resonance imaging (MRI) has been used (Miller JM, et al. *IOVS* 2004;45:ARVO E-Abstract 2388),[9–11] to provide pictorial representations of sections through the living eye at multiple positions, from which a detailed investigation of ocular dimensions can be made.

In a previous article, we described the linear dimensions of emmetropic and myopic eyes.[11] Adult emmetropes and myopes (up to −12 D) were examined with a clinical MRI scanner. Eye length was measured from anterior cornea to retina, and height and width were measured from retina to retina. Amid considerable intersubject variation, the length of most emmetropic eyes (23.0 ± 0.7 mm) was more than the height (22.4 ± 1.0 mm) or width (22.7 ± 0.9 mm). As myopic refractive corrections increased, eyes became larger in all three dimensions, but more so in length (mean 0.35 mm/D) than height (0.19 mm/D) and more so in height than width (0.10 mm/D).

Although this study[11] provided considerable information about the relationship of the ocular dimensions to the degree of myopia, how the shape of the retinal surface changes with myopia was not described. This information is important for understanding imaging in the eye's periphery. In addition, there is much speculation as to whether the type and magnitude of peripheral refractive errors play a role in the development of myopia. It has been hypothesized that a very steep retinal shape may predispose a young emmetropic eye toward elongation, because the "hypermetropic" peripheral retina may stimulate compensating eye growth[12] (see Fig. 1, top and middle). The fact that young emmetropic and hypermetropic pilots with hypermetropic refraction shifts in the periphery are more prone to the development of myopia than are those showing myopic shifts in the periphery supports this suggestion.[13] Subsequent ophthalmic correction of the central myopia that develops may promote further progression by causing the peripheral retina to become relatively hypermetropic once more (Fig. 1, bottom).

Different interpretations of what is meant by ocular shape has led to confusion in this area. Some studies inferred eye shape from the overall size of the eye—that is, including anterior and posterior segments (Miller JM, et al. *IOVS* 2004; 45:ARVO E-Abstract 2388),[1–4,11] or from the overall appearance of eyes.[9,14] Other indirect estimates of eye shape have been based on peripheral refraction results. On average, emmetropic eyes show slight myopic refractive shifts from the central retina to the periphery, whereas uncorrected hypermetropes have greater relative myopic shifts, and uncorrected myopes have either relative hypermetropic shifts[6,15,16] or smaller myopic shifts than emmetropes.[17] Starting with the assumption that the emmetropic eyes are generally spherical in shape, Mutti et al.[6] concluded that to account for the peripheral refraction trends, hypermetropes would generally have oblate eyes (steeper in the periphery than at the fovea) and myopes would generally have prolate eyes.

Another interpretation of ocular shape relates to the shape of the retina. One study by Chen et al.[10] made a direct determination of retinal shape in a small number of subjects, while Schmid[5] made an indirect determination from differences in eye length along different visual field angles. Chen et al.[10] measured departures from circularity of the transverse axial sections of retinas of three hypermetropic, four emmetropic, and four myopic eyes; the hypermetropic retinas had only small departures from circularity, the emmetropic retinas were found to be prolate (flatter in the periphery than at the fovea), and the myopic retinas yet more prolate. Schmid[5] found, based on relative differences in central (on-axis) and peripheral (15°) eye length, that children with myopic eyes have steeper retinas than those with emmetropic eyes. This would tend to make

From the [1]Centre for Health Research—Optometry and the [2]School of Physical and Chemical Sciences, Queensland University of Technology, Brisbane, Queensland, Australia.

Supported by National Health and Medical Research Council Grant 199912 (DAA, KLS).

Submitted for publication December 20, 2004; revised February 27, 2005; accepted March 26, 2005.

Disclosure: **D.A. Atchison**, None; **N. Pritchard**, None; **K.L. Schmid**, None; **D.H. Scott**, None; **C.E. Jones**, None; **J.M. Pope**, None

The publication costs of this article were defrayed in part by page charge payment. This article must therefore be marked "*advertisement*" in accordance with 18 U.S.C. §1734 solely to indicate this fact.

Corresponding author: David A. Atchison, School of Optometry, QUT, Kelvin Grove Q 4059, Australia; d.atchison@qut.edu.au.

myopic eyes appear elongated, but Cheng et al.[9] and Chau et al.[14] did not find this to be the case.

Because the shape of the retina is of potential importance in understanding the development of myopia, in this study we use ellipsoid modeling of the retinal surface of ocular MRIs to determine the retinal shapes of a large group of emmetropic and myopic eyes. We also took the opportunity to measure lens tilts and retinal–choroidal and scleral thicknesses, as these would be necessary for the development of more accurate anatomically based emmetropic and myopic eye models.

METHODS

Participants

The research adhered to the tenets of the Declaration of Helsinki, with the research approved by the Human Research Ethics Committees of both the Queensland University of Technology (QUT) and the Prince Charles Hospital, and informed consent obtained from all participants. The participants were 21 emmetropes (best spherical corrections −0.50 to +0.75 D) and 66 myopes (−0.75 D to −12.00 D), aged 18 to 36 years (mean, 25.5), with small amounts of astigmatism (≤0.75 D) except for five subjects (astigmatism, 1.00–2.00 D). Best spherical corrections (mean spherical equivalents) were determined by subjective refractions (two examiners) in the spectacle plane. The right eye was used unless it was outside the refraction range or acuity was reduced because of amblyopia; seven left eyes were used in the study. Eighty-seven of 88 participant image pairs were used in the calculation of retinal shape (one participant had only an axial image). Sixty percent of participants were female.

Eighty four percent and 16% of our participants were white and Asian, respectively, with 2 (10%) of emmetropes and 12 (18%) of myopes being Asian. There were too few nonwhite participants to make any meaningful analysis of racial differences. It is possible that our findings were influenced by the racial distribution of our participants.

Collection of MRIs

The methodology for obtaining the magnetic resonance images has been described previously,[11] but some details are given herein. Participants were positioned supine in a clinical MRI scanner (Twin Speed, 1.5 Tesla; General Electric, Milwaukee, WI), using a 7.5-cm receive-only radio surface coil positioned over the eye. The contralateral eye was occluded. An LED fixation target was imaged straight ahead of the subject by an overhead 45° inclined mirror. Transverse axial (horizontal through the middle of the eye) and sagittal (vertical through the visual axis) sections were taken with a T_1-weighted fast spin-echo (FSE) sequence, with the following parameters: receiver bandwidth, ±15 kHz; slice thickness, 3 mm; field of view, 80 × 80 mm; pulse flip angle, 90°; repetition time (TR), 400 ms; echo time (TE), 16.9 ms; echo train length, 4; four averages; and acquisition matrix, 320 × 320 (interpolated with zero-filling to 512 × 512). Acquisition time was 130 seconds. Sagittal FSE images were acquired with fat suppression to minimize the chemical shift artifact in the inferior region of the sclera.

Ellipsoid Fits of the Retinal Surface

We developed a software program to calculate the retinal shape as an ellipsoid, using the orthogonal magnetic resonance images (DICOM format, 512 × 512 pixels, and 16-bit, gray-scale resolution). Through the program's graphic user interface, a subject's image set was loaded and displayed. Due to small misalignment of the fixation target of 3.2° (right eyes) and 3.6° (left eyes) when measurements were made, the transverse axial images were corrected by rotating them by these amounts. The transverse axial images of the left eye images were then flipped horizontally to match right eye images. The operator used the cursor to identify the approximate locations of four major points within each image. In the sagittal images these were the lens center, the fovea, and the superior and inferior retinal edges. For transverse axial images these were the lens center, the fovea, and the temporal and nasal retinal edges. Accurately locating these major points was not necessary. Each image was cropped and low-pass filtered using a pixel-wise adaptive Wiener method, which is based on statistics estimated from a local 3 × 3 neighborhood around each pixel. Edge detection was performed by the Canny method, which is based on

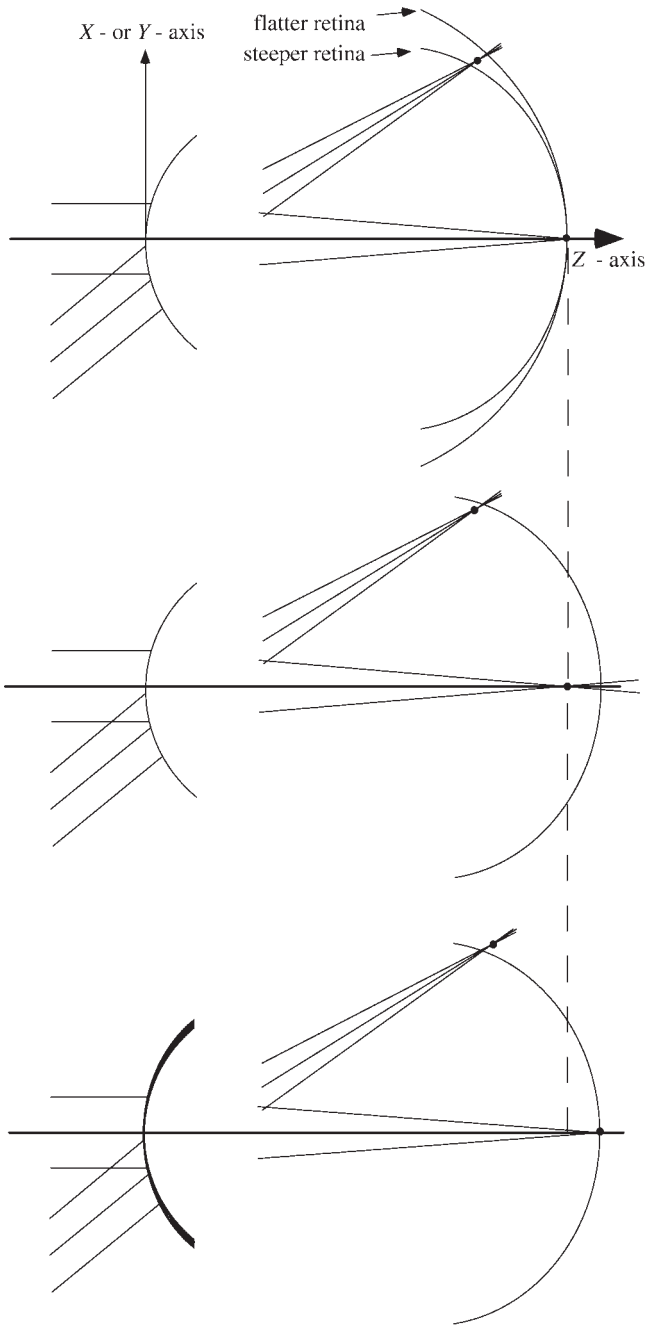

FIGURE 1. Possible schema for the development of myopia. *Top*: an emmetropic eye with two alternate retinal shapes: one relatively flat and one relatively curved. Light from an off-axis point converges to focus in front of the flatter retina (relative myopia), but toward a point behind the steeper retina (relative hypermetropia). *Middle*: the eye with the steeper retina responds to the peripheral relative hypermetropia by elongating. *Bottom*: a negative-power correcting lens (shown as a contact lens, *bold curve*) restores the relative hypermetropia in the periphery, thus restarting the cycle. For the purposes of the figure, peripheral astigmatism was ignored.

searching for local maxima in the gradient of the given image. Pixels from the retinal region were culled if they lay outside an angle that subtended 120° either side of the visual axis with respect to a center of the eye, defined by the four major points just listed, so that 60% to 70% of the retinal perimeter was used for analysis (Fig. 2).

There were two populations of edge pixels: those belonging to the lens and those belonging to the retina. In the final stage of segmentation, the operator was able to manipulate these pixel populations manually, to ensure the boundaries were represented as accurately as possible. Using the cursor, the operator could add or remove edge pixels. Once the retinal and lens boundaries were defined, a third coordinate of image section depth was added to the pixels so that they were defined in three-dimensional Cartesian space, with the necessary coordinate reassignments made to ensure pixels from corresponding sections combined in a unified manner.

Ellipses were fitted to the segmented pixel data in each image using a least-squares approach. These provided an initial estimate of ellipsoidal parameters. Ellipsoids were fitted through the data, one for the retinal boundary and another for the lens boundary. The fitting was achieved using multidimensional unconstrained nonlinear minimization with the iterative Nelder-Mead procedure. In each iteration, an ellipsoid was constructed for a given parameter set, and the root mean square (RMS) error calculated between the ellipsoid and data points. The RMS provided a goodness-of-fit measure for each ellipsoid calculation. The Nelder-Mead procedure was used to manipulate the ellipsoid's parameters until the RMS error was minimized. The final RMS was used as the measure of quality of the final ellipsoids.

The ellipsoids had the function

$$\frac{x'^2}{R_{x'}^2} + \frac{y'^2}{R_{y'}^2} + \frac{(z' - R_{z'})^2}{R_{z'}^2} = 1,$$

where $R_{x'}$, $R_{y'}$ and $R_{z'}$ were the semidiameters of the ellipsoid along the final x', y', and z' axes.

An alternative way of describing the ellipsoids is in terms of vertex curvatures, $c_{x'v}$ and $c_{y'v}$, and asphericities, $Q_{x'}$ and $Q_{y'}$. For the x'-z' principal sections

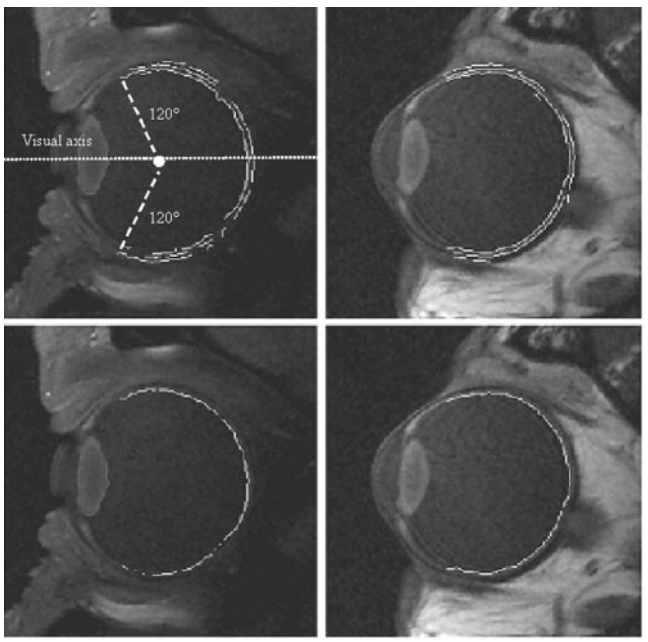

FIGURE 2. Example of an edge-detection result for sagittal (*left*) and axial (*right*) images, before (*top*) and after (*bottom*) the investigator's input.

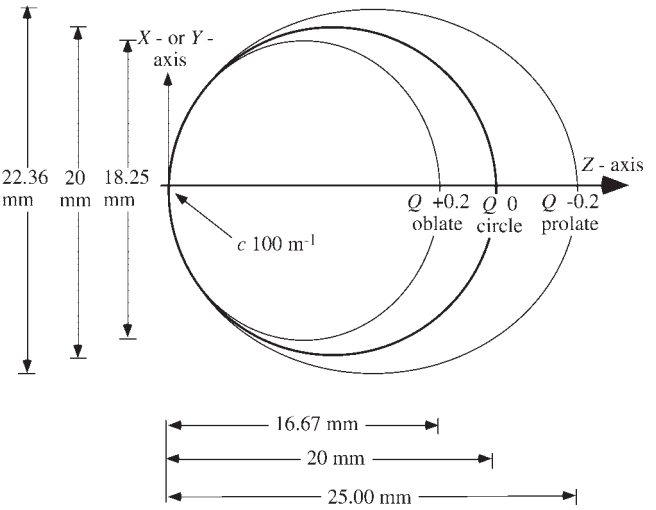

FIGURE 3. Sample ellipses with the same vertex curvature. The horizontal and vertical dimensions, vertex curvature, and Q values are shown.

$$c_{x'v} = \frac{R_{z'}}{R_{x'}^2} \text{ and } Q_{x'} = \frac{R_{x'}^2}{R_{z'}^2} - 1$$

and for the y'-z' principal sections

$$C_{y'v} = \frac{R_{z'}}{R_{y'}^2} \text{ and } Q_{y'} = \frac{R_{y'}^2}{R_{z'}^2} - 1.$$

If $Q_{x'}$ was positive, the projection of an ellipsoid along the x'-z' section (an ellipse) steepened away from the vertex and was referred to as oblate. This corresponded to $R_{x'}/R_{z'}$ as greater than 1. If $Q_{x'}$ was zero, the ellipse reduced to a circle, and if $Q_{x'}$ was negative, the ellipse flattened away from the vertex and was referred to as prolate. The situation was similar for the y'-z' section (Fig. 3).

The orientations and positions of the ellipsoids can be realized through a rotation θ_z about the z-axis, θ_y about the y-axis, and θ_x about the x-axis, performed in that sequence. These are followed by decentrations x_c in the x direction (horizontal), y_c in the y direction (vertical), and z_c in the z direction (parallel to the visual axis).

Other Measurements

Other measurements were made that are relevant to the modeling of emmetropic and myopic eyes. Lens tilts were calculated with the same program that determined retinal shapes. Measures of retinal–choroidal and scleral thicknesses were made directly in approximately 40% of eyes from the transverse axial and sagittal images at both the fovea and at the transverse and sagittal equators. (The choroidal and scleral boundaries were unclear in the other eyes.) The nasal plus the temporal thickness was determined using the method previously described,[11] so that approximately half this dimension represents the transverse equatorial thickness. Similarly, the sagittal equatorial thickness was determined. Also, we determined an "anterior segment" depth from the differences between the length measurements of the eye, based on transverse axial images[11] and the lengths of retinal ellipsoids ($2R_{z'}$).

Statistical Analysis

In this article, summary statistics are provided for ellipsoid parameters and differences between ellipsoid and ellipse asphericities of both emmetropes and myopes. Data are expressed as the mean ± SD and 95% confidence interval (CI) of the mean. To determine the association of ellipsoid parameters with degree of myopia, linear regressions were

performed for each parameter with refractive correction. Ellipsoid parameters were compared to the corresponding ellipse parameters by a method used for evaluating repeatability.[18,19] Additional one-sample *t*-tests were used to indicate whether the total group means of some parameters were significantly different from zero. In all tests, $P < 0.05$ were considered significant.

Results

Retinal Ellipsoid Shapes and Sizes

The mean ellipsoid of the retinal shape of the emmetropic group had considerably more width and height than length (i.e., it was oblate). It had x', y', and z' dimensions of 11.40 ± 0.47, 11.18 ± 0.50, and 10.04 ± 0.49 mm, respectively (Table 1). For all but one emmetrope, $x'$and y' dimensions were larger than the z' dimension.

With an increase in degree of myopia, the z' dimension increased more quickly than the x' and y' dimensions (Fig. 4a). The z' semidiameter increased by 0.16 mm/D of myopia, the y' by 0.09 mm/D, and the x' by 0.04 mm/D (Table 1). The z' and y' semidiameters correlated significantly with refractive correction (Table 1). The x' semidiameter is close to correlating significantly with refractive correction ($P = 0.067$; Table 1).

The mean asphericities $Q_{x'}$ and $Q_{y'}$ of retinal ellipsoids for emmetropes were +0.30 ± 0.11 and +0.25 ± 0.11, respectively. As myopia increased, the retinas became less oblate, more so in the x'-z' (horizontal) than in the y'-z' (vertical) principal sections (Fig. 4b). Most of the myopic eyes had oblate shapes, with only 8 of 66 myopic eyes being prolate (having negative asphericity) in either principal section. These eyes had refractions of −1, −3.25, −3.25, −5.625, −6.25, −6.375, −7.25, and −7.50 D, and so were well spread across the myopic range. The most negative asphericity (−0.09) was close to zero (spherical). Although oblateness decreases with the increase in myopia, even with 10 D of myopia, few eyes can be expected to be prolate (i.e., have flattening ellipsoids).

Figure 4c shows vertex curvatures $c_{x'v}$ and $c_{y'v}$ of the ellipsoids in the x'-z' and y'-z' principal sections, respectively, as a function of refractive correction. For emmetropes, the mean $c_{x'v}$ and $c_{y'v}$ were 77.4 ± 5.3 and 80.6 ± 6.8 m^{-1}, respectively. As with the previous parameters, there was considerable interindividual variability. The $c_{x'v}$ increased significantly by 0.64 m^{-1} for each diopter of myopia (adjusted $R^2 = 0.047$, $P = 0.024$), but $c_{y'v}$ did not change significantly with degree of myopia (Table 1).

Retinal Ellipsoid Rotation and Decentration

Ellipsoid vertices were rotated generally nasal to and above ellipsoid centers. For emmetropes, mean θ_x, θ_y, and θ_z were +1.2 ± 6.7° (a positive value indicates that the vertex is above the ellipsoid center), +11.0 ± 7.0° (a positive value means that the vertex is nasal to the ellipsoid center) and +0.01 ± 0.07°, respectively (Table 1). Only mean θ_y was significantly different from zero ($t = 7.18$, $P < 0.001$). The small variation of θ_z from zero is to be expected because the ellipsoid fits were determined from transverse axial and sagittal sections. Figure 5a shows the ellipsoid rotations θ_x, θ_y, and θ_z of the retinal ellipsoids as a function of refractive correction. Although neither θ_x nor θ_y changed significantly with myopia, both mean θ_x and θ_y of the total group were now significantly different from zero (+3.6 ± 11.2°, $t = 3.03$, $P = 0.003$ and +11.5 ± 13.2°, $t = 8.15$; $P < 0.001$, respectively). It is interesting to compare θ_y for the retina with that for the lens. For emmetropes, mean θ_y of the retinal ellipsoid was +11.0 ± 7.0° compared with +4.0 ± 2.4° for the lens ellipsoid—that is, the retinal tilt was nearly three times that of the lens. Lens tilt was not significantly influenced by degree of myopia (adjusted $R^2 = -0.001$, $P = 0.348$).

For emmetropes, mean decentrations x_c and y_c of the ellipsoid centers were −0.41 ± 0.30 mm (negative means decentration nasal to fovea) and −0.19 ± 0.35 mm (negative means decentration below the fovea), respectively, and both were significantly different from zero ($t = 6.2$, $P < 0.001$; $t = 2.5$, $P = 0.023$, respectively). Figure 5b shows the decentrations x_c and y_c of ellipsoid centers as a function of refractive correction. Neither x_c nor y_c changed significantly with refractive correction (Table 1). Mean x_c and y_c of the total group were −0.51 ± 0.37 and -0.23 ± 0.48 mm and were significantly different from zero ($t = 12.8$, $P < 0.001$; $t = 4.3$, $P < 0.001$, respectively).

Gender Differences

A comparison between the men and the women was made because men have bigger eyes than women. The emmetropic men had mean semidiameters in the principal meridians that were approximately 0.4 mm larger than those of the women. Changes in the dimensions with refraction were similar in both sexes. Asphericities $Q_{x'}$ and $Q_{y'}$ were similar in the male and female emmetropes and changes in the asphericities with refraction were similar in both genders. The female emmetropes had vertex curvatures greater than did the male emmetropes by approximately 3.8 and 4.6 m^{-1} in the x'-z' and y'-z' sections (both corresponding to smaller vertex radii of curvature of approximately 0.5 mm). For neither gender did the vertex curvatures change significantly with refraction (unlike the total group in the x'-z' section). Of interest is that the mean radius of curvature in the two sexes in the principal meridians were 0.5 to 1.2 mm greater than the 12.0 mm often used as the radius in model eyes,[20] although because of oblate shapes, approximately 70% of retinas of the total group had semidiameters in both the x' and y' meridians that were < 12.0 mm.

Differences between Ellipsoids and Ellipses

The principal sections of the ellipsoids did not always correspond closely to the transverse axial (horizontal) and sagittal (vertical) image sections, particularly the former (Fig. 5a). As measurements of various parameters (e.g., peripheral refraction) are sometimes measured in the horizontal and vertical meridians, we were interested in how the ellipsoid measurements might compare with the fitted ellipses in the image sections. Figure 6 shows the differences between ellipsoid and ellipse asphericities plotted as a function of their averages. Generally small differences were found, although there were some outliers. In both the horizontal and vertical sections, the mean differences between ellipsoid and ellipse asphericities were small at 0.02 ± 0.06 and −0.01 ± 0.06 mm, respectively, although both were significantly different from zero ($t = 2.9$, $P = 0.004$; $t = -2.2$, $P = 0.029$, respectively). In view of the generally small differences between the three- and two-dimensional results, the parameters for the former can be taken as applying to the relevant horizontal or vertical section through the fovea in our study group.

Goodness of Fit and Repeatability

Mean ± SD of the RMS error of the fits were 0.67 ± 0.21 mm with a range of 0.42 to 1.63 mm. The RMS was independent of refractive correction (adjusted $R^2 = 0.002$, $P = 0.29$). The higher RMS values corresponded to images of poorer quality or with asymmetry in the transverse axial and/or sagittal sections. Another way of considering goodness of fit is to compare differences between direct measurements of the diameters[11] and the ellipse diameters. In both the transverse axial and sagittal sections, the mean differences were small (−0.07 ±

Table 1. Linear Regression Analysis Results for Ellipsoid Parameters and Other Ocular Dimensions, as a Function of Refractive Correction

	Ellipsoid Data of Total Group			Emmetropic Retinal Surface Data			Myopic Retinal Surface Data			
Parameter	**Intercept**	**Slope**	**Adj. R^2**	***P***	**Mean ± SD**	**Range**	**95% CI**	**Mean ± SD**	**Range**	**95% CI**
Retinal ellipsoid radii (mm)										
x'	11.455	−0.043	0.028	0.067	11.40 ± 0.47	10.67–12.39	11.19–11.61	11.61 ± 0.55	10.33–13.03	11.48–11.75
y'	11.365	−0.090	0.153	0.000	11.18 ± 0.50	10.24–11.95	10.95–11.41	11.72 ± 0.50	10.52–13.14	11.60–11.84
z'	10.148	−0.163	0.385	0.000	10.04 ± 0.49	9.30–11.03	9.82–10.26	10.72 ± 0.59	9.38–12.21	10.58–10.87
Retinal ellipsoid asphericity										
$Q_{x'}$	0.279	0.028	0.264	0.000	0.30 ± 0.11	0.06–0.53	0.25–0.35	0.18 ± 0.12	−0.06–0.55	0.15–0.21
$Q_{y'}$	0.258	0.018	0.129	0.000	0.25 ± 0.11	−0.11–0.42	0.20–0.30	0.20 ± 0.12	−0.09–0.52	0.17–0.23
Retinal ellipsoid curvature at vertex (m^{-1})										
$c_{x'v}$	77.639	−0.636	0.047	0.024	77.37 ± 5.26	68.41–85.84	74.98–79.76	77.37 ± 5.26	68.41–85.84	78.18–81.47
$c_{y'v}$	78.891	0.019	−0.012	0.944	80.57 ± 6.77	72.84–101.79	77.49–83.65	80.57 ± 6.77	72.84–101.79	76.86–79.73
Retinal ellipsoid rotation (°)*										
$\theta_{x'}$	2.276	−0.545	0.003	0.272	1.17 ± 6.73	−21.27–9.69	−1.89–4.23	4.43 ± 12.22	−24.28–43.99	1.42–7.43
$\theta_{y'}$	9.558	−0.780	0.009	0.181	10.97 ± 7.00	1.83–27.93	7.78–14.16	11.69 ± 14.64	−28.51–45.03	8.09–15.28
$\theta_{z'}$	0.021	0.003	−0.006	0.492	0.01 ± 0.07	−0.21–0.12	−0.02–0.04	0.02 ± 0.09	−0.16–0.46	−0.00–0.04
Lens tilt (°) horizontal	4.469	0.100	−0.001	0.348	4.01 ± 2.37	1.26–8.68	2.93–5.09	4.28 ± 2.43	−3.83–9.35	3.68–4.88
Retinal ellipsoid decentration (mm)†										
x_c	−0.503	0.004	−0.011	0.806	−0.41 ± 0.30	−0.95–0.11	−0.55–−0.27	−0.54 ± 0.39	−1.52–0.52	−0.64–0.45
y_c	−0.242	−0.007	−0.011	0.757	−0.19 ± 0.35	−0.83–0.38	−0.35–−0.03	−0.24 ± 0.52	−1.38–1.35	−0.36–−0.11
"Anterior segment" i.e. AL–2*$R_{z'}$ (mm)	3.033	−0.015	−0.009	0.609	2.96 ± 0.57	1.35–3.83	2.70–3.22	3.11 ± 0.66	1.39–4.82	2.94–3.27

Data include 21 emmetropic eyes and 66 myopic eyes with a refractive correction range from −0.75 to −12.00 D. y = slope · x + intercept. Adj., adjusted.

* Positive rotation indicates that the vertex is above/nasal to the ellipsoidal center.

† Positive decentration indicates that the ellipsoid center is above/temporal to the fovea.

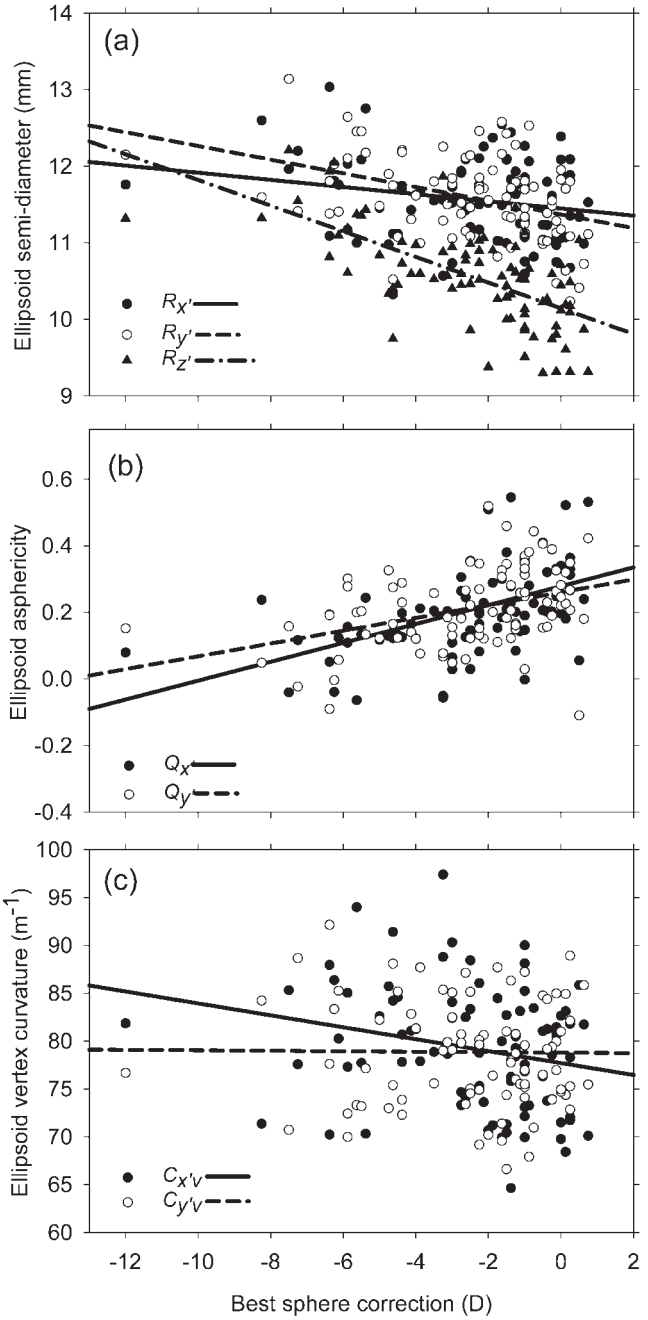

FIGURE 4. Effect of refractive correction on ellipsoid dimensions. (**a**) Semidiameters, (**b**) asphericities, and (**c**) vertex curvatures of the ellipsoids fitted to the retina are plotted as a function of the best sphere correction. Linear regression fits are given in Table 1.

0.28 and +0.05 ± 0.23 mm, respectively), although the former was significantly different from zero ($t = -2.16$, $P = 0.03$). The corresponding ranges were −0.91 to +0.68 and −0.70 to +0.56 mm.

The repeatability of the investigator's input to the retinal shape determination (i.e., edge identification), was minimal and test–retest evaluation on 10 eyes showed mean absolute differences of 0.03 to 0.11 mm (0.23%–0.87%) across the three major semidiameters.

Retinal–Choroidal and Scleral Thicknesses

In the emmetropes, both the retinal–choroidal and scleral thicknesses were generally similar at the posterior pole and at the equators (Table 2). With increased myopia, the retinal–choroidal thickness at the equator decreased significantly, both at the horizontal equator (0.020 mm/D) and at the posterior pole (0.014 mm/D), but not vertically at the equator, and the sclera thickness decreased significantly only at the posterior pole, with the regression slope of 0.035 mm/D predicting that thickness would halve at 10 D myopia. There was also a tendency for thinning at the horizontal equator.

"Anterior Segment" Depth

The mean "anterior segment" depth for emmetropes was 2.96 ± 0.57 mm. Figure 7 shows depths as a function of refractive correction. These segment depths did not change significantly with refraction, and the mean depth of the total group was 3.07 ± 0.64 mm.

Discussion

Major Findings

We fitted nonrotationally symmetric ellipsoids to the retinal surfaces of 87 emmetropic and myopic eyes. Nearly all the emmetropic retinas were oblate in shape in both transverse axial and sagittal sections, meaning that the retina surfaces steepened away from the posterior retinal vertex in all meridians and had more width and height than length. With increased myopia up to 12.0 D, retinas were less oblate in shape, but only 12% of myopic retinas were prolate in shape (flatten-

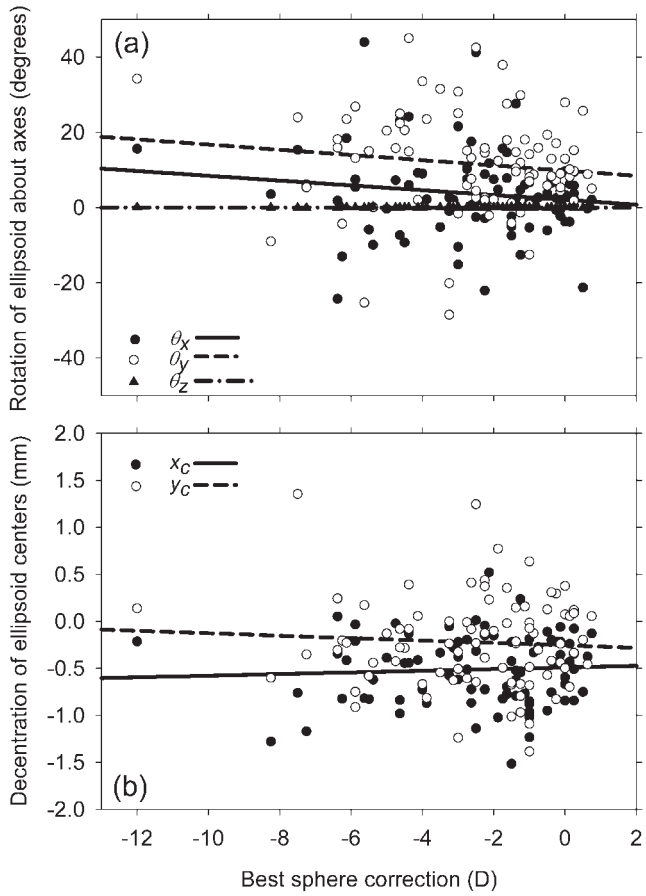

FIGURE 5. Effect of refractive correction on ellipsoid position. (**a**) Axis rotations of fitted ellipsoids (θ_x, θ_y, θ_z) and (**b**) decentrations of the ellipsoid centers (x_c, y_c) are plotted as a function of the best sphere correction. Linear regression fits are given in Table 1.

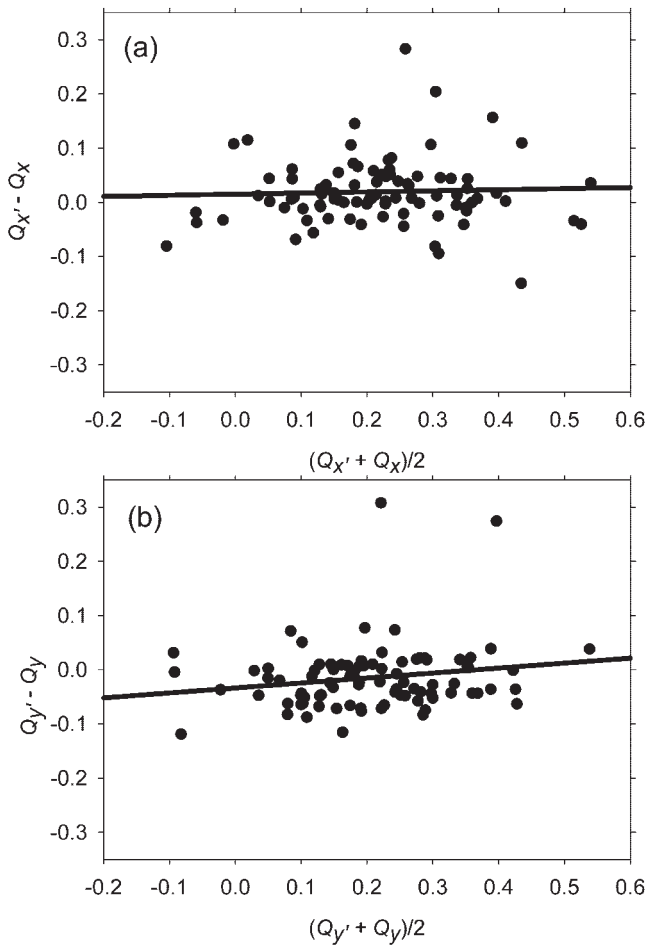

FIGURE 6. Comparison between ellipsoid and ellipse parameters. Differences between asphericities of ellipsoids and ellipses are plotted as a function of the average of the two asphericities. (**a**) $Q_{x'}$ (ellipsoid) and Q_x (ellipse); (**b**) $Q_{y'}$ (ellipsoid) and Q_y (ellipse). The regression equation for $Q_{x'} - Q_x$ is $y = 0.02x + 0.02$, adjusted $R^2 = -0.010$, $P = 0.699$; and the regression equation for $Q_{y'} - Q_y$ is $y = 0.09x - 0.03$, adjusted $R^2 = 0.020$, $P = 0.098$.

ing away from the posterior pole with greater length than width or height) in either transverse axial or sagittal sections. Our findings support those of Chau et al.[14] that eye shape obtained with MRI "challenges the notion that the eyeball is elongated in myopia, at least within the range of −12.00 D."

Other noteworthy findings are that the ellipsoids were tilted around the vertical axis by approximately 11° and their centers were decentered horizontally by 0.5 mm nasally relative to the visual axis (this finding was the same in emmetropes and the total study group). The mean retinal tilt was in the same direction as, but nearly three times greater than, the mean tilt of the eye lenses. The mean retinal tilt was more than two times the angle α—the angle between the visual axis and the best fit to the optical axis—which is considered to be approximately 5°.[20] This finding is at least a partial explanation of asymmetries in peripheral refraction along the horizontal visual field.[15–17,21–24]

Comparison with Previous Studies

To our knowledge, the only study of retinal shape with which our results can be directly compared is that of Chen et al.[10] who made MRI measurements in the transverse axial section and presented results for three hypermetropes, four em-

TABLE 2. Linear Regression Analysis Results for Retinal-Choroidal and Scleral Thicknesses, as a Function of Refractive Correction

Parameter	Linear Regression				Emmetropic Dimensions				Myopic Dimensions			
	Intercept	Slope	Adj. R^2	P	n	Mean ± SD	Range	95% CI	n	Mean ± SD	Range	95% CI
Retinal–choroidal thickness (mm)												
Nasal + temporal	0.977	0.020	0.050	0.033	22	0.99 ± 0.23	0.72–1.51	0.88–1.09	50	0.91 ± 0.17	0.56–1.34	0.86–0.96
Superior + inferior	0.894	−0.002	−0.018	0.884	13	0.86 ± 0.14	0.62–1.08	0.78–0.95	42	0.91 ± 0.20	0.00–1.37	0.85–0.97
Posterior	0.672	0.014	0.050	0.024	22	0.70 ± 0.15	0.45–1.13	0.63–0.76	61	0.62 ± 0.12	0.38–1.06	0.59–0.65
Scleral thickness (mm)												
Nasal + temporal	0.796	−0.017	0.020	0.120	22	0.75 ± 0.14	0.52–1.17	0.68–0.81	50	0.87 ± 0.24	0.47–1.54	0.81–0.94
Superior + inferior	0.702	0.009	−0.008	0.452	13	0.71 ± 0.10	0.54–0.88	0.65–0.77	42	0.67 ± 0.21	0.00–1.15	0.61–0.74
Posterior	0.746	0.035	0.127	0.001	22	0.73 ± 0.27	0.40–1.23	0.61–0.85	61	0.63 ± 0.21	0.26–1.41	0.58–0.68

Data include 21 emmetropic eyes and 66 myopic eyes with a refractive correction range from −0.75 to −12.00 D. y = slope · x + intercept. Adj., adjusted.

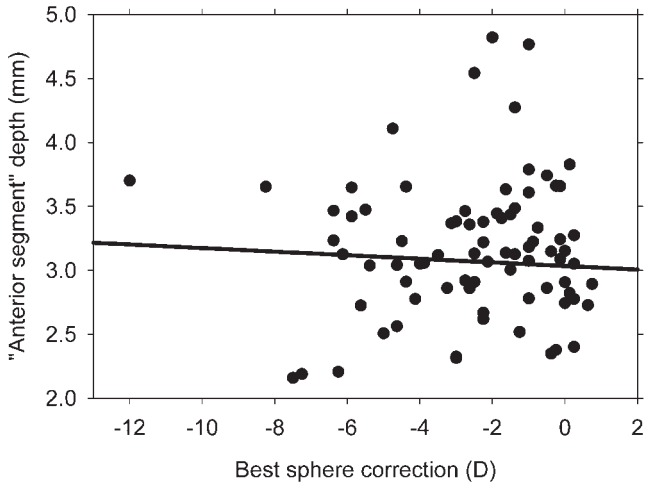

FIGURE 7. Effect of refractive correction on anterior segment depth. The linear regression fit is given in Table 1.

metropes, and four myopes. They found the best-fitting circles to the retina for each subject and determined the distances of several points on the retina from this circle. They divided this distance by the radius of the circle. The distance/radius was plotted as a function of angle around the circle. In hypermetropes, the ratios were close to one at most retinal positions. However, myopes and emmetropes had ratios greater than one at the fovea and less than one at the equators, indicating prolate shapes. The variations in the ratios indicate asphericities (Q) of the emmetropic retinas and three of four myopic eyes as being within the approximate range -0.2 to -0.3. Our findings contradict those of Chen et al.,[10] as we found oblate retinal shapes in most emmetropic and myopic eyes. The results of Chen et al.[10] had inferior magnetic resonance image quality. With the advantage of improvements in MRI technology we were able to use an MRI system and imaging protocol that provided higher resolution images of the eye, allowing a more accurate estimation of retinal boundary. Checks were also made to ensure that the system was free of artifacts that might cause imaging distortions,[11] which Chen et al. do not appear to have done.[10] This is crucial because poor "shimming" and hence poor homogeneity of the static magnetic field and/or poor gradient linearity can give rise to image distortions that could easily make the eye appear prolate rather than oblate.

TABLE 3. Dimensions of the Model Eye for an Emmetrope and a 10-D Myope for the Horizontal and Vertical Sections

Parameter	Emmetrope	10-D Myope
Corneal radius (mm)	7.7	7.7
Anterior segment (mm)	3.1	3.1
Ellipsoid decentration H/V (mm)	−0.5/−0.2	−0.5/−0.2
Ellipsoid rotation H/V (°)	+11/+3.6	+11/+3.6
Asphericity Q H/V	+0.27/+0.25	+0.02/+0.08
Ellipsoidal diameter (mm)	22.91/22.73	23.78/24.53
Ellipsoidal length (mm)	20.30	23.56

H, horizontal; V, vertical

Cheng et al.[9] made MRI measurements of ocular dimensions in seven myopes, six emmetropes, and eight hypermetropes. They did not measure retinal shape but axial distances (cornea to outer sclera) and equatorial distances both horizontally and vertically (outer sclera to outer sclera). When the thicknesses of the retina-choroid and sclera are subtracted from their measurements and some protrusion of the corneas from the retinal envelope are taken into account, at least most of their hypermetropic, emmetropic, and myopic retinas are oblate in shape. Thus, their data are consistent with our findings.

Proposed Retinal Shape Model

Previous optical modeling of myopia has included an equatorial diameter that is unaffected by the degree of myopia.[25,26] In the light of our results, the equatorial diameter must increase, particularly in the vertical meridian. In one model of myopia the retinal shape remained constant, with the location of the equator moving away from the cornea as myopia increased,[25] whereas in the other model the retinal surface became more prolate but the equator was fixed relative to the cornea.[26] The anterior segment depth, the difference between the length of the eye and the length of the retinal ellipse, did not change as a function of refraction (Fig. 7), suggesting that a good model for the retinal shape of myopic eyes has its anterior vertex fixed, with the equator moving away from the cornea at half the rate that the posterior retina moves away from the cornea.

Based on our measurements, ellipsoidal models of emmetropic and 10-D myopic retinas were constructed. A cornea with a 7.7-mm radius of curvature was placed 3.1 mm from the front vertex (the corneal radius may change with myopia, but is fixed in this model). The dimensions of the model retinas are shown in Table 3 and Figure 8. These models, in both the

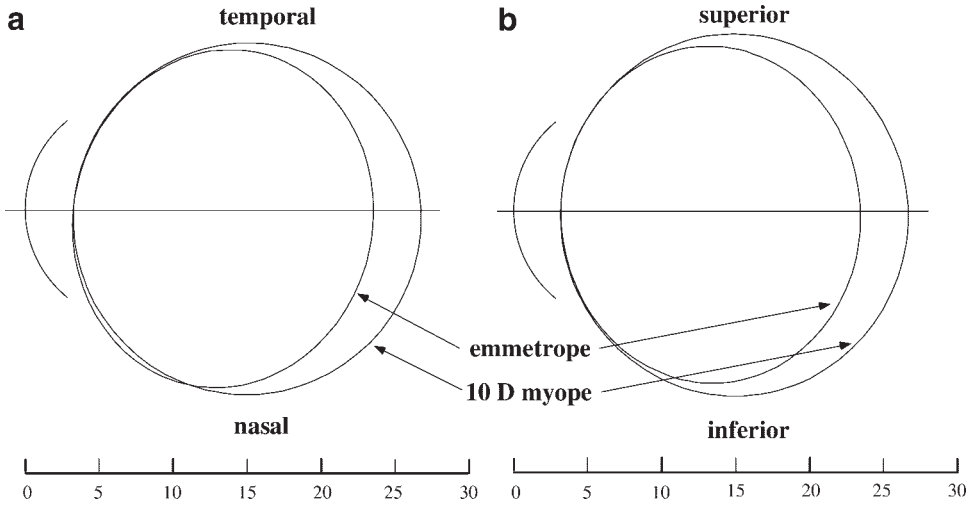

FIGURE 8. Models of average emmetropic and 10 D myopic eyes in the horizontal (*a*) and vertical sections (*b*). The parameters of these models are shown in Table 2.

horizontal (Fig. 8a) and vertical sections (Fig. 8b), demonstrate the oblate shape of the emmetropic retina, along with the decrease in oblateness in the highly myopic retina. Although the width of the ellipsoids was not significantly dependent on degree of myopia ($P = 0.067$, Table 1), we used it in our model, as eye width measured directly from the MRI image was significantly dependent on myopia in our previous study.[11]

In a previous publication, we discussed three mechanisms of stretching in myopia[11]: equatorial elongation, global elongation, and posterior polar elongation. The equatorial elongation model has the length but not the width and height increasing, and the global elongation model gives proportional increases in the three dimensions and hence no change in asphericity. The posterior polar model has changes taking place in a restricted region at the back of the eye. We do not know what is happening in any single eye, but our model is intermediate between the equatorial and global expansion models by having differential growth in different meridians. A closer inspection of our data over a limited region might be used to investigate the posterior polar elongation model, but we do not expect this to give any insights because of the generally good fits of the ellipsoids (see goodness of fit and repeatability in the Results section) and we did not see evidence of posterior staphylomas in any of the images.

Retinal–Choroidal and Scleral Thicknesses

This model of a retina expanding from a fixed anterior position may be applied to predict retinal–choroidal and scleral thickness changes. Assuming the volume of tissue remains unchanged with increased myopia, the retina-choroid and sclera should gradually thin toward the back of the eye, with differential meridional effects according to the stretching in different meridians (e.g., thinner along the vertical than along the horizontal direction). The model is successful for the sclera, in which the thickness only decreased significantly with increased myopia at the posterior pole (Table 2). However, the model is not successful for the retina-choroid. With increase in myopia, the retina-choroid thinned at the equator horizontally (0.02 mm/D) but not vertically, and it thinned less at the posterior pole (0.014 mm/D) than at the horizontal equator (Table 2).

Cheng et al.[9] found that their small group of myopes (-7 ± 3 D) had five ninths the posterior retinal-choroidal thickness and two thirds the posterior scleral thickness as did their emmetropes, which is broadly in line with our findings.

Study Limitations

One limitation of the study concerns the ability to identify appropriate transverse axial and sagittal sections from pilot MRI scans. On the sagittal scans, some manipulation of the mirror above the volunteer's head when viewing the fixation target was made so that the tested eye appeared to be looking upward, and this judgment was influenced largely by the eye lens orientation. We are thus unable to make any reliable estimates of vertical lens tilts, and the tilts of the retinas in the vertical direction (Table 1) are relative to the lens tilt in this direction. The value usually given to the angle α in the vertical direction is –2° (optical axis downward toward the retina), and this must suffice as a likely error in the orientation of the sagittal imagery. Our choice of visual axis was based on the center of the lens, as the iris was generally too indistinct for its center to be determined accurately, and so this does not take into account any lens decentrations relative to the pupil center. Another limitation is that the ellipsoid fits were based on two image sections. A more thorough analysis would include more orientations through the eye or many parallel sections. This would increase the time considerably beyond the 130 seconds to acquire each image, and increase the likelihood that eye and head movements would degrade the image quality, but with technological advances more detailed measurements and sophisticated fitting might be possible.

There was a gap in refraction of 3.75 D between the highest myope and the next highest myope. Removing the highest myope (12 D) from regression analyses had only small influences on fitting coefficients and no influence on their significances.

Implication for Progression of Myopia

Our data clearly show that most myopes have oblate, rather than prolate, retinal shapes (even up to 12 D). Both the off-axis power of the optics of the eye and the position of the retinal surface influence whether the retinal periphery is relatively hypermetropic or not. Our data suggest that the relative hyperopic shifts in the retinal periphery of myopes measured with off-axis refraction techniques are not due to prolate retinal shapes. Other important factors are likely to be the change in axial length and changes in corneal shape. We intend to test this further with optical modeling.

Conclusion

Both emmetropic and myopic retinas are usually oblate in shape. An oblate retinal shape may have implications for research investigating development of myopia.

Acknowledgments

The authors thank Michael Statham and the radiography staff of the MRI unit at Prince Charles Hospital for assistance with data collection.

References

1. Deller JFP, O'Connor AD, Sorsby A. X-ray measurements of the diameters of the living eye. *Proc R Soc Lond B Biol Sci*. 1947:456–467.
2. Zhou X-D, Wang F-R, Zhou S-Z, Shi J-S. A computed tomographic study of the relation between ocular axial biometry and refraction. In: Tokoro T, ed. *Proceedings of the 6th International Conference on Myopia, Kakone-machi, Japan.* Tokyo: Springer; 1998:112–116.
3. Vohra SB, Good PA. Altered globe dimensions of axial myopia as risk factors for penetrating ocular injury during peribulbar anaesthesia. *Br J Anaesth*. 2000;85:242–245.
4. Meyer-Schwickerath G, Gerke E. Biometric studies of the eyeball and retinal detachment. *Br J Ophthalmol*. 1984;68:29–31.
5. Schmid GF. Axial and peripheral eye length measured with optical low coherence reflectometry. *J Biomed Opt*. 2003;8:655–662.
6. Mutti DO, Sholtz RI, Friedman NE, Zadnik K. Peripheral refraction and ocular shape in children. *Invest Ophthalmol Vis Sci*. 2000;41:1022–1030.
7. Walker TW, Mutti DO. The effect of accommodation on ocular shape. *Optom Vis Sci*. 2002;79:424–430.
8. Logan NS, Gilmartin B, Wildsoet CF, Dunne MC. Posterior retinal contour in adult human anisomyopia. *Invest Ophthalmol Vis Sci*. 2004;45:2152–2162.
9. Cheng HM, Singh OS, Kwong KK, Xiong J, Woods BT, Brady TJ. Shape of the myopic eye as seen with high-resolution magnetic resonance imaging. *Optom Vis Sci*. 1992;69:698–701.
10. Chen J, Elsner A, Burns S, et al. The effect of eye shape on retinal responses. *Clin Vis Sci*. 1992;7:521–530.
11. Atchison DA, Jones CE, Schmid KL, et al. Eye shape in emmetropia and myopia. *Invest Ophthalmol Vis Sci*. 2004;45:3380–3386.
12. Wallman J, Winawer J. Homeostasis of eye growth and the question of myopia. *Neuron*. 2004;43:447–468.
13. Hoogerheide J, Rempt F, Hoogenboom WPH. Acquired myopia in young pilots. *Ophthalmologica*. 1971;163:209–215.

14. Chau A, Fung K, Pak K, Yap M. Is eye size related to orbit size in human subjects? *Ophthalmic Physiol Opt*. 2004;24:35–40.
15. Millodot M. Effect of ametropia on peripheral refraction. *Am J Optom Physiol Opt*. 1981;58:691–695.
16. Atchison DA, Pritchard N, White SD, Griffiths AM. Influence of age on peripheral refraction. *Vision Res*. 2005;45:715–720.
17. Seidemann A, Schaeffel F, Guirao A, Lopez-Gil N, Artal P. Peripheral refractive errors in myopic, emmetropic, and hyperopic young subjects. *J Opt Soc Am A*. 2002;19:2363–2373.
18. Bland JM, Altman DG. Statistical methods for assessing agreement between two methods of clinical measurement. *Lancet*. 1986;1:307–310.
19. Bland JM, Altman DG. Measuring agreement in method comparison studies. *Stat Methods Med Res*. 1999;8:135–160.
20. Atchison DA, Smith G. *Optics of the Human Eye*. Oxford, UK: Butterworth-Heinemann; 2000.
21. Rempt F, Hoogerheide J, Hoogenboom WPH. Peripheral retinoscopy and the skiagram. *Ophthalmologica*. 1971;162:1–10.
22. Lotmar W, Lotmar T. Peripheral astigmatism in the human eye: experimental data and theoretical model predictions. *J Opt Soc Am*. 1974;64:510–513.
23. Dunne MCM, Misson GP, White EK, Barnes DA. Peripheral astigmatic symmetry and angle alpha. *Ophthalmic Physiol Opt*. 1993;13:303–305.
24. Gustafsson J, Terenius E, Buchheister J, Unsbo P. Peripheral astigmatism in emmetropic eyes. *Ophthalmic Physiol Opt*. 2001;21:393–400.
25. Charman WN, Jennings JAM. Ametropia and peripheral refraction. *Am J Optom Physiol Opt*. 1982;59:922–923.
26. Dunne MCM, Barnes DA, Clement RA. A model for retinal shape changes in ametropia. *Ophthalmic Physiol Opt*. 1987;7:159–160.